Exploring multi-band excitations of interacting Bose gases in a 1D optical lattice by coherent scattering

Xinxing Liu,[1] Xiaoji Zhou,[1,*] Wei Zhang,[2] Thibault Vogt,[1] Bo Lu,[1] Xuguang Yue,[1] and Xuzong Chen[1]

[1]*School of Electronics Engineering and Computer Science, Peking University, Beijing 100871, P.R. China*
[2]*Department of Physics, Renmin University of China, Beijing 100872, P.R. China*
(Dated: January 19, 2013)

We use a coherent Bragg diffraction method to impart an external momentum to ultracold bosonic atoms trapped in a one-dimensional optical lattice. This method is based on the application of a single light pulse, with conditions where scattering of photons can be resonantly amplified by the atomic density grating. An oscillatory behavior of the momentum distribution resulting from the time evolution in the lattice potential is then observed. By measuring the oscillating frequencies, we extract multi-band energy structures of single-particle excitations with zero pseudo-momentum transfer for a wide range of lattice depths. The excitation energy structures reveal the interaction effect through the whole range of lattice depth.

I. INTRODUCTION

Cold atomic gases loaded in optical lattices have drawn great attention in the past few years as a versatile and powerful experimental system to study strongly correlated many-body problems [1]. By taking advantage of great controllability and perfectness, this novel type of matter features a promising candidate to achieve some important modeling systems and help tackling many unaddressed questions in multi-disciplinary fields of physics. As an example, important progress has been made in manipulation and characterization of interacting bosons loaded in an optical lattice, both for the low-lattice/low-temperature Bose-Einstein condensate (BEC) regime and for the high-lattice/high-temperature Mott Insulator (MI) or normal regime [2–8].

Among these efforts, the understanding of excitations gives crucial information about the underlying system, for its ability to characterize the system's response in different regimes. For shallow lattices, the gas behaves as superfluid and the excitation spectrum can be described by the Bogoliubov theory within a mean-field description of interaction effect. For deep lattices, the gas enters the strongly correlated MI phase, where the excitation exhibits a gap at low energies. Experimental characterization of these features include the measurement of first band effective mass by Bloch oscillation [9], the demonstration of gap in the MI regime [3], and the momentum-resolved probe of multi-band dispersion by Bragg spectroscopy [10–15].

In this manuscript, we report a novel experimental scheme to detect multi-band excitation with zero quasi-momentum transfer for interacting bosons loaded in a one-dimensional (1D) optical lattice across a wide range of lattice depth. The elementary excitations are created
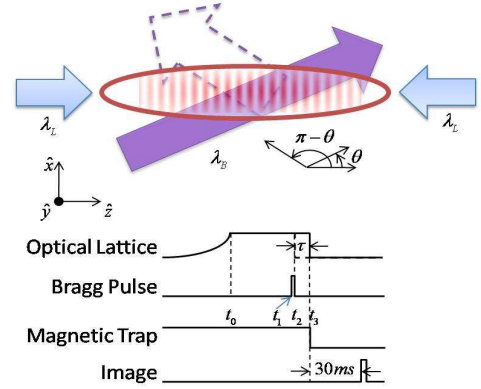

FIG. 1: (Color online)Schematic setup (top) and time sequence (bottom) of our experimental scheme. After loading the BEC in a 1D optical lattice with an exponential ramp (40 ms), a laser beam of $5\mu s$ is sent at $\theta = 24°$ from the longitudinal axis, and is scattered into a symmetrical direction according to the Bragg scattering condition. After holding the lattice potential for another duration of τ, both the lattice and the magnetic trap are abruptly switched off and an absorption image is taken after a time-of-flight (TOF) of 30 ms.

using Bragg scattering, where light waves are scattered collectively in accommodation to the periodic distribution of bosonic atoms. As a response to this coherent process, the atoms will recoil with a momentum in unit of the reciprocal lattice, and can be excited to higher energy bands with the same pseudo-momentum. By monitoring the time evolution of the momentum distribution, we can extract information about the excitation energy. In shallow lattices where gases are superfluid, we can get the ($n = 1$) as well as the ($n = 2$) band excitation energy. For deep lattices where the ground state is a MI, the large band gap prohibits dramatic population to higher

*Electronic address: xjzhou@pku.edu.cn

band, such that only the ($n = 1$) band excitation energy is obtained. Throughout the whole range of lattice depth variation, we also observe a sizable signature of interaction effect, due to the large occupation number for each lattice site.

We stress that our scheme is different from Bragg spectroscopy, where atoms are excited by a direct transfer of energy and momentum via a two-photon process stimulated by two distinct laser beams [10–15]. In Bragg spectroscopy, the two laser beams form an effective one-dimensional optical lattice moving along a specified direction. If we see from the lattice frame, the atoms which are stationary in the lab frame are moving along the opposite direction, and the Bragg spectroscopy scheme corresponds to an effective diffraction of atomic wave function on this optical grating. Therefore, this procedure usually requires a coherence condition for atoms and a beam duration of milliseconds to achieve distinct diffraction peaks, which corresponds to significant population of specific excited states.

In contrast, our experimental scheme involves only one incident beam, and the periodic density distribution of atoms in optical lattices are considered as gratings, from which the photons are scattered and cooperatively amplified given a certain geometry to fulfill the Bragg scattering condition. Therefore, this method does not rely on phase coherence of atoms in different sites, and can be directly applied to the MI/normal regime. Besides, as the speed of photon is c, the building up time of scattering light field is negligible and this optically coherent process requires a much shorter light beam duration only in scale of microseconds, hence brings less heating or other complications to the atomic system.

Our paper is organized as follows. In Sec. II we describe the experimental scheme based on the application of a single Bragg diffraction pulse on a gas loaded in a one dimensional lattice. In Sec. III we present our results on the oscillatory behavior of the momentum distribution observed as a function of keep time in the optical lattice after applying the Bragg pulse. Sec. IV is devoted to a more careful analysis of Bragg diffraction obtained with a single light pulse and used as a tool throughout this experiment. This diffraction is revisited with semi-classical theory and an interpretation in terms of collective light scattering; In Sec. V, we summarize our work and draw conclusion.

II.   EXPERIMENTAL DESCRIPTION

The experimental setup and protocol is illustrated in Fig.1. We first prepare a BEC of about 2×10^5 ^{87}Rb atoms in a QUIC trap, with longitudinal length $L = 100$ μm and transverse length $l = 10$ μm. The BEC is then loaded into a 1D optical lattice $V_{ol}(x) = V[1 + \cos(2k_L x)]/2$ along its axial direction by an adiabatic ramping of 40 ms. Here, V is the lattice depth, and $k_L = 2\pi/\lambda_L$ is the reciprocal lattice spacing with λ_L the
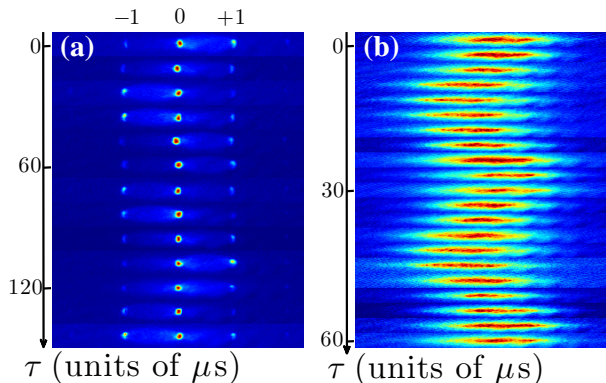

FIG. 2: (Color online) (a) TOF images for $V = 12E_R$. From top to bottom, the holding time τ increases from zero with a step of 12μs. An oscillatory behavior of the first order peaks at $\pm 2\hbar k_L$ can be clearly observed. (b) Similar results for $V = 37E_R$. Although the interference pattern is wiped out and no peaks is present, the oscillation of the momentum distribution can be still determined.

lattice light wavelength. After holding the lattice for 50 ms, we shine the Bragg pulse from a certain direction θ (see Fig. 1). The beam is red-detuned by $\delta = 1.3$ GHz from the $(5S_{1/2}, F = 2) \rightarrow (5P_{3/2}, F' = 3)$ transition, and for a typical duration of $\Delta t = t_2 - t_1 = 5$ μs. After the Bragg pulse, we further hold the system for a certain amount of delay time τ, and suddenly shut down all the trapping potentials to get time-of-flight (TOF) images which are taken after 30 ms of free expansion process.

Due to the presence of the optical lattice, the atoms are initially distributed into an array of quasi-two-dimensional slices, which are separated equidistantly by the lattice spacing $\lambda_L/2 = 426$ nm. For each slice of atoms, the Bragg pulse incident from the direction of θ will be *reflected* to the direction of $(\pi - \theta)$, such that the optical lengths of different light paths are the same. Besides, the coherent condition for diffraction also requires the optical length difference between light paths scattered from adjacent slices is a multiple of the Bragg beam wavelength λ_B. In our case of $\lambda_B = 780$ nm, these coherent conditions single out a specific incident direction of the Bragg pulse with $\cos\theta = \lambda_B/\lambda_L$, only at which significant collective scattering of light could occur.

As a consequence of cooperative scattering (cf. Sec. IV), the photons would exert a recoil momentum of $2\hbar k_L$ to the atoms, leading to the occupation of different states with various bands but zero quasi momentum. After that, the momentum distribution experience an obvious oscillation due to the presence of optical lattices. This oscillation can be observed from a series TOF images by varying the holding time τ. One typical result for $V = 12E_R$ is shown in Fig. 2(a), where the system is in the BEC regime and a clear oscillation of the occupation number of particles in $p = \pm 2\hbar k_L$ is observed. In Fig. 2(b), we also present a similar result for $V = 37E_R$, where the high lattice potential destroys the phase co-

herence and the system becomes a normal gas. Notice that although the interference patterns no longer exist in the TOF images, the momentum oscillation can still be clearly determined.

III. RESULTS AND ANALYSIS

For shallow lattices where the system is in the BEC phase, atoms are macroscopically distributed in the lowest quantum state which is described by the Gross-Pitaevskii (GP) equation

$$\left[-\frac{\hbar^2\partial_x^2}{2m} + V_{\text{ol}}(x) + V_{\text{ext}}(x) + U_0|\Psi(x)|^2\right]\Psi(x) = \mu\Psi(x),$$
(1)

where $V_{\text{ext}}(x) = m\omega_x^2 x^2/2$ is the external harmonic trap, $U_0 = 4\pi\hbar^2 a_s/m$ is the interaction with a_s the s-wave scattering length, and μ is the chemical potential. In the mean field level, the repulsive interaction acts as an effective potential $U_0 n_0(x)$ with n_0 the condensate fraction, which tends to reduce the height of the optical lattice. This combined effective lattice $V_{\text{eff}}(x) = V_{\text{ol}}(x) + U_0 n_0(x)$ has the same period as the original one, and forms a band structure for single particle state. The presence of BEC ensures that only the state at the band bottom is macroscopically occupied. This state is characterized by the band index $(n = 0)$ and pseudo-momentum $(q = 0)$, denoted by

$$\Psi(x, t_1) = \phi_{n=0, q=0}(x) = \sum_R W_{n=0}(x - R), \quad (2)$$

where $\phi_{n,q}(x)$ is the Bloch state, $W_n(r)$ is the Wannier function, and the summation over R runs over all lattice sites. After the Bragg pulse, an external momentum of $2\hbar k_L$ is transferred to the atoms. As this momentum transfer is resonant with the reciprocal lattice, there should be no new pseudo-mementum state being excited, and the system is described by

$$\begin{aligned}\Psi(x, t_2) &= \sum_n a_n \phi_{n, q=0}(x) \\ &= L^{-1/2}\sum_{n,\ell} a_n c_{n,q=0}^\ell e^{i2\ell\hbar k_L x}, \end{aligned} \quad (3)$$

where $c_{n,q}^\ell = \langle 2\ell\hbar k_L|\phi_{n,q}\rangle$ is the projection of the Bloch state to the plane wave state with momentum $2\ell\hbar k_L$, and a_n is determined by the intensity and duration of the Bragg beam. Here, we should emphasize that the Bloch states $\phi_{n,q}(x)$ with $q = 0$ are periodic functions of $\lambda_L/2$, hence can be further expanded by a series of plane waves with ℓ being integers.

After the Bragg pulse, the wavefunction $\Psi(x, t)$ evolves in the presence of the optical lattice as

$$\begin{aligned}\Psi(x, t_2 + \tau) &= \sum_n a_n \phi_n(x) e^{iE_n\tau} \\ &= L^{-1/2}\sum_\ell e^{i2\ell\hbar k_L x}\sum_n a_n c_n^\ell e^{iE_n\tau}. \end{aligned} \quad (4)$$

Here, we have dropped the subscript $(q = 0)$ for simplify notation, and E_n is the corresponding eigenenergy of the nth band. In realistic conditions, the summation over n is restricted to $n \leq 2$ due to negligible population of higher bands. Therefore, the average momentum $\langle p \rangle = \langle\Psi(t)|p|\Psi(t)\rangle$ and the atom number in the ℓth momentum mode N_ℓ would acquire oscillatory behavior

$$\begin{aligned}\frac{\langle p \rangle}{2\hbar k_L} &= C_{10}\cos(\omega_{10}\tau + \varphi_{10}) \\ &\quad + C_{21}\cos(\omega_{21}\tau + \varphi_{21}), \end{aligned} \quad (5)$$

$$\begin{aligned}\frac{N_\ell - \overline{N_\ell}}{N_{\text{tot}}} &= D_{10}^\ell\cos(\omega_{10}\tau + \varphi_{10}) + D_{20}^\ell\cos(\omega_{20}\tau + \varphi_{20}) \\ &\quad + D_{21}^\ell\cos(\omega_{21}\tau + \varphi_{21}), \end{aligned} \quad (6)$$

where the three frequencies correspond to the energy gaps of $\omega_{10} = (E_1 - E_0)/\hbar$, $\omega_{20} = (E_2 - E_0)/\hbar$, and $\omega_{21} = (E_2 - E_1)/\hbar$, respectively, as illustrated in Fig. 3(c). Notice that the frequency $\omega_{20} = (E_2 - E_0)/\hbar$ is not present in the oscillation of $\langle p \rangle$. This is because the momentum distribution of states in bands $(n = 0)$ and $(n = 2)$ are both even symmetric, hence make no net contribution to $\langle p \rangle$. The coefficients C's and D's are determined by

$$\begin{aligned}C_{nm} &= 2|a_m^* a_n|\sum_\ell \ell c_m^\ell c_n^\ell, \\ D_{nm}^\ell &= 2|a_m^* a_n| c_m^\ell c_n^\ell, \end{aligned} \quad (7)$$

the initial phase factors are determined by $\varphi_{nm} = \text{angle}(a_m^* a_n)$, the N_{tot} is the total atom number and the time average of N_ℓ is $\overline{N_\ell} = \sum_n |a_n|^2 |c_n^\ell|^2 N_{\text{tot}}$.

Given the expressions of Eqs (5) and (6), we can extract the three frequencies from evolution of the average momentum $\langle p \rangle$ [Fig. 3(a)], and the relative number of particles in $p = -2\hbar k_L$ state [Fig. 3(b)] via a fitting process, as depicted with solid (red) curves. One should notice that since the frequency ω_{21} is relatively small, it would require longer evolution time τ to be precisely determined. Considering the typical range of $\tau \lesssim 250\mu$s in our experimental scheme, a more practical strategy is to fit the other two frequencies ω_{10} and ω_{20} first, and rely on the relation $\omega_{21} = \omega_{20} - \omega_{10}$ to get ω_{21}.

In Fig. 4, we show the results of oscillating frequencies of ω_{10} and ω_{20} for various optical lattice depths ranging from 8 to 37 E_R. Notice that the frequency ω_{20} can only be obtained for lattice depth $V \leq 16E_R$, as the strong lattice potential prohibits significant excitation to the $(n = 2)$ band. For shallow lattices with $V \lesssim 25E_R$, the system is in the BEC regime presenting clear interference pattern in the TOF images, and the discussion above remains valid. If we neglect the interaction effect between atoms, the band structure can be calculated based on the bare optical lattice potential, and the mutual gaps between different bands are indicated as solid lines. As one would expect, this estimation is systematically above our experimental observation, since the repulsive interaction tends to reduce the lattice depth to a lower effective value.
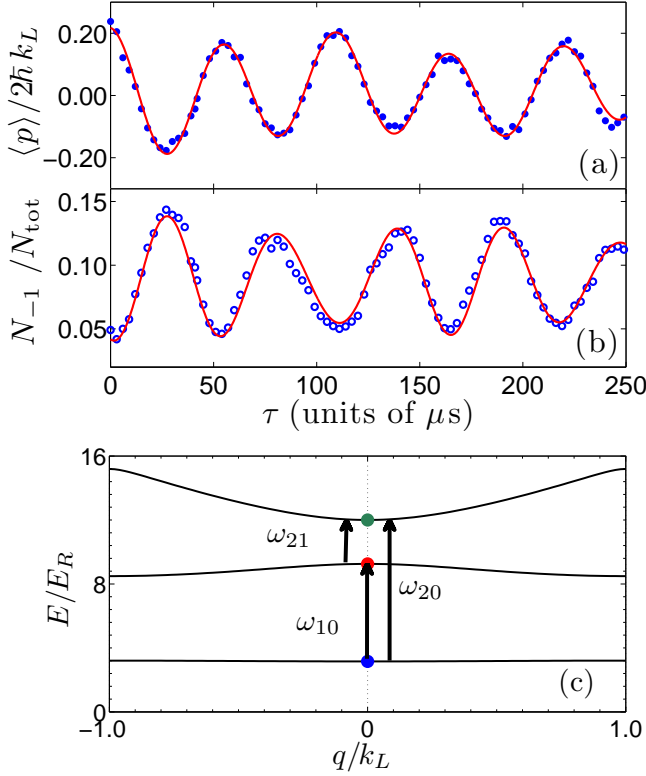
FIG. 3: (Color online) From the TOF images, we can extract (a) the average momentum of the cloud and (b) the relative occupation number of the -1 order with $p = -2\hbar k_L$. By fitting the results with Eqs. (6) and (5) (red solid), we can extract the frequencies between multi energy bands, as schematically drawn in (c). The results correspond to the case of $V = 12E_R$, and all date points are taken as average of more than three experimental trails.

One theory to incorporate the interaction effect is discussed in Ref. [16], where Choi and Niu analyzes the interaction effect for the bottom ($n = 0$) band and gives an approximate expression for the effective potential $V_{\text{eff}} = V/(1 + 4C)$ by assuming a nearly uniform condensate distribution. Here, $C = \pi n_0 a_s / k_L^2$ is the dimensionless interaction strength and n_0 the *average* three-dimensional condensate density. By using the effective potential, the oscillating frequencies can be extracted as mutual gaps between different bands, as illustrated in Fig. 4 (dashed lines). Another method to capture the interaction effect is to use a tight-binding model [17], which is more reasonable for deeper lattices since the Wannier functions for all bands are well localized within one lattice site. Thus, we can calculate the bottom and first exited band structures via a variational method by neglecting higher order overlaps between sites, and extract the frequency ω_{10} (dotted line in Fig. 4). We emphasize that neither of the theories above has included finite temperature nor inhomogeneity effect, and their comparison to our experimental data can only be understood to a qualitative level.
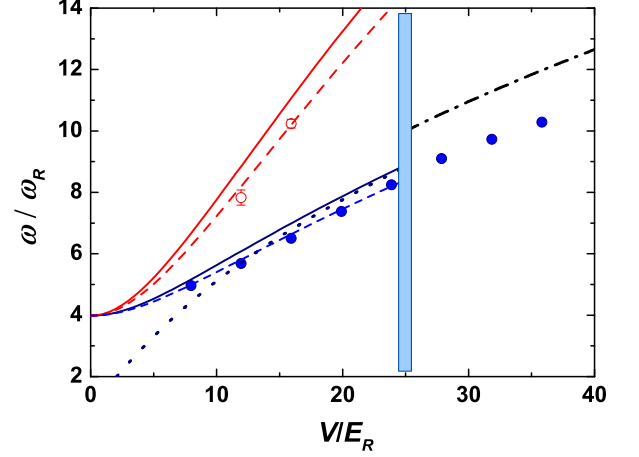

FIG. 4: (Color online) Oscillating frequencies ω_{10} (solid dots) and ω_{20} (hollow dots) in the unit of recoiled frequency $\omega_R = E_R/\hbar$. In the BEC regime with $V \leq 25E_R$ (left), experimental results are systematically below the bare lattice calculation (solid), where interaction effect is not taken into account. To incorporate the interaction effect, an effective potential theory (dashed) and a tight-binding model (dotted) are considered. In the MI/normal regime with $V > 25E_R$ (right), the oscillating frequency ω_{10} is compared with the trapping frequency of the lattice potential (dashed-dotted), where we use $a_s = 4.7$ nm, and $n_0 = 10^{14}$ cm^{-3}.

Up to now, we have restricted our discussion to the shallow lattices regime where the system is in the BEC phase. By further increasing the lattice height over 25 E_R, the strong local confinement would eventually break the global phase coherence between different sites, and the system leave the BEC regime. In this case, since the recoil energy from diffracted photons $E_B = 4E_R$ is much smaller than the confining potential, atoms that are kicked by the Bragg pulse are mainly localized within one lattice site and swing to and fro around the site center. If we neglect the interaction effect, the oscillating frequency is thus the trapping frequency of the lattice potential, as shown in Fig. 4 (dashed-dotted line). Notice that this bare lattice estimation is significantly above the experimental measurements. A detailed description of the interaction effect would require a solution of the hydrodynamic equation, which is beyond the scope of the present manuscript.

IV. SEMICLASSICAL THEORY FOR THE COOPERATIVE SCATTERING PROCESS

Finally, we notice that the oscillating frequencies between different energy bands can be identified only for fairly deep optical lattices with $V \geq 8E_R$. For shallower lattices, we could not observe significant oscillation. This can be easily understood by reminding that the incident
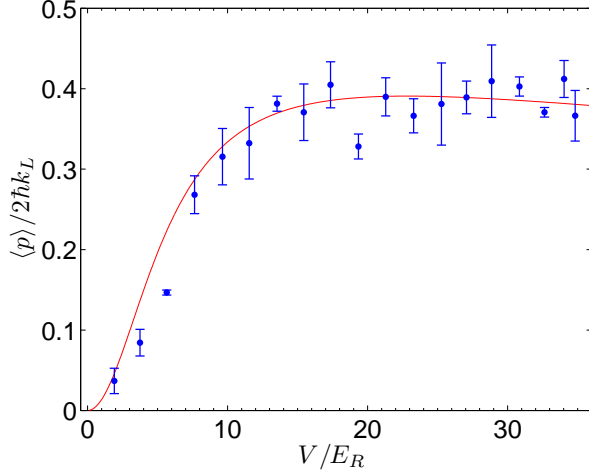
FIG. 5: (Color online) Average momentum of the cloud from TOF images upon released from the trap *right* after the Bragg pulse of 5 μs. Each data point is an average of more than three experimental trials. This result can be well described by a semiclassical theory (solid, see text), with fitting coupling constant $g = 0.9$ MHz.

photons are coherently scattered and amplified by the atomic grating, which becomes more apparent in deeper lattice potentials. This scattering processes can be described by using a semiclassical theory [18]. We start with the Maxwell-Schrödinger equation, which describes the evolution of atomic wave function $\Psi(x,t)$ and the positive and negative frequency components of the classical electric field $\mathbf{E}^{(\pm)}$:

$$i\hbar\frac{\partial}{\partial t}\Psi(x,t) = \hat{H}\Psi + \frac{(\mathbf{d}\cdot\mathbf{E}^{(-)})(\mathbf{d}\cdot\mathbf{E}^{(+)})}{\hbar\delta}\Psi(x,t), \quad (8)$$

$$\frac{\partial^2\mathbf{E}^{(\pm)}}{\partial t^2} = c^2\nabla^2\mathbf{E}^{(\pm)} - \frac{1}{\varepsilon_0}\frac{\partial^2}{\partial t^2}\mathbf{P}^{(\pm)}. \quad (9)$$

where $\hat{H} = -\frac{\hbar^2}{2M}\nabla^2 + V(x)$ the single atom Hamiltonian, δ the detuning of the laser from the electronic transition, $\mathbf{d}$ the atomic dipole moment, and $\mathbf{P}^{(\pm)} = -\frac{|d|^2|\Psi|^2}{\hbar\delta}\mathbf{E}^{(\pm)}$ the polarization. By decomposing the atomic wave and electric field as $\Psi = \sum_{\ell}\Psi_{\ell}e^{i\cdot 2\ell k_L x}$, and $\mathbf{E}^{(\pm)} = \varepsilon_p^{\pm}e^{-i(\omega_p - k_L x - k_z z)} + \varepsilon_s^{\pm}e^{-i(\omega_s + k_L x - k_z z)}$, we can get:

$$\frac{\partial}{\partial t}\Psi_{\ell} = \frac{-i|d|^2}{\hbar^2\delta}\left(|\varepsilon_p^+|^2\Psi_{\ell} + \varepsilon_p^+\varepsilon_s^-\Psi_{\ell-1} + \varepsilon_s^+\varepsilon_p^-\Psi_{\ell+1}\right),$$
$$(10)$$

$$\frac{\partial\varepsilon_s^+}{\partial t} + c\frac{\partial\varepsilon_s^+}{\partial x_s} = \frac{-i|d|^2\omega_s}{2\varepsilon_0\hbar\delta}\left(\sum_{\ell}|\Psi_{\ell}|^2\varepsilon_s^+ + \sum_{\ell}\Psi_{\ell}\Psi_{\ell+1}^*\varepsilon_p^+\right),$$
$$(11)$$

where ε_p and ε_s are the amplitude of the pumping light and the scattered light, ω_p and ω_s are the corresponding frequencies, k_z is the wave vector perpendicular to

the lattice light, x_s is the coordinate along the direction of the scattered beam. The second term of Equation (10)'s right side represents that an atom at $\Psi_{\ell-1}$ absorb a photo from the pumping Bragg beam and emit another into the scattered beam. During this process it receives recoiled momentum of $2\hbar k_L$ and is transmitted into Ψ_{ℓ} mode. On the other hand, the third term shows an atom from $\Psi_{\ell+1}$ mode absorb a photo from the scattered beam and emit one into the pumping beam and is transferred backward into Ψ_{ℓ} mode. Equation (11) shows the evolution and propagation of the scattered beam. Note that it is the atomic grating $\sum_{\ell}\Psi_{\ell}\Psi_{\ell+1}^*$ that initially transfers photons into the scattered beam from the pumping light.

Assuming that the amplitude of light field varies slowly, and neglecting the spatial distribution of Ψ_{ℓ} and $\varepsilon_s^{\pm}$ [19], we get:

$$\frac{\partial\tilde{c}_{\pm 1}}{\partial t} = \pm g(\tilde{c}_{\mp 1}^*\tilde{c}_0 + \tilde{c}_0^*\tilde{c}_{\pm 1})\tilde{c}_0, \quad (12)$$

$$\frac{\partial\tilde{c}_0}{\partial t} = g(|\tilde{c}_{-1}|^2 - |\tilde{c}_1|^2)\tilde{c}_0, \quad (13)$$

where $\tilde{c}_{\ell}(t) = \langle 2\ell\hbar k_L|\Psi(t)\rangle$, the amplitude of ℓth momentum mode, can be solved numerically from the above equations, together with the initial conditions $\tilde{c}_{\ell}(0) = c_{n=0}^{\ell}$. $g = |d_{12}|^4|\varepsilon_p|^2\omega_s nL/(2\epsilon_0 c\hbar^3\delta^2)$ represent the coupling of the light with BEC of length L. Using the relation $\tilde{c}_{\ell} = \sum_n c_n^{\ell}a_n$ we can determine the coefficients a_n and their evolution, hence obtain the oscillation process discussed above. In Fig. 5, we show the average momentum $\langle\hat{p}\rangle = 2\hbar k_L\sum_{\ell}\ell\cdot|\tilde{c}_{\ell}|^2$ of the cloud right after a Bragg pulse of 5μs duration, and compare with the semiclassical prediction. For shallow lattices, the momentum change is relatively small such that the oscillatory behavior upon time evolution is blurred. However, for deeper lattice potentials, significant amount of momentum can be transferred to atoms via this coherent scattering process.

V. CONCLUSION

In summary, an experimental investigation of multiband energy spectrum for a bosonic system loaded in a 1D optical lattice is demonstrated. A coherent Bragg light scattering process to excite atoms to higher energy bands with zero pseudo-momentum transfer, and oscillatory behavior of average momentum upon holding the sample of atoms in the optical lattice for various evolution times, are first reported. We extract the oscillating frequencies, which correspond to the energy gap between different bands, for a wide range of lattice potential depth. Throughout the whole range of lattice depth, we observe the effect of repulsive interaction between particles, which tends to reduce the lattice height to a lower effective value. Our method is a coherent process where photons are scattered and amplified by the atomic density grating, while the previously reported Bragg spectroscopy requires a high coherence of atoms.

[1] I. Bloch and M. Greiner, Adv. At. Mol. Opt. Phys. **52**, 1 (2005).

[2] M. Geriner, O. Mandel, T. Esslinger, T.W. Hänsch, and I. Bloch, Nature **415**, 39 (2002).

[3] T. Stöferle, H. Moritz, C. Schori, M. Köhl, and T. Esslinger, Phys. Rev. Lett. **92**, 130403 (2004).

[4] B. Paredes, A. Widera, V. Murg, O. Mandel, S. Fölling, I, Cirac, G.V. Shlyapnikov, T.W. Hänsch, and I. Bloch, Nature **429**, 277 (2004).

[5] T. Kinoshita, T. Wenger, and D.S. Weiss, Science **305**, 1125 (2004).

[6] J. K. Chin, D.E. Miller, Y. Liu, C. Stan, W. Setiawan, C. Sanner, K. Xu, and W. Ketterle, Nature **443**, 961 (2006).

[7] Z. Hadzibabic, P. Kruger, M. Cheneau, B. Battelier, and J. Dalibard, Nature **441**, 1118 (2006).

[8] I. B. Spielman, W.D. Phillips, and J.V. Porto, Phys. Rev. Lett. **98**, 080404 (2007).

[9] O. Morsch, J.H. Müller, M. Cristiani, D. Ciampini, and E. Arimondo, Phys. Rev. Lett. **87**, 140402 (2001).

[10] M. Kozuma, L. Deng, E.W. Hagley, J. Wen, R. Lutwak, K. Helmerson, S.L. Rolston, and W.D. Phillips, Phys. Rev. Lett. **82**, 871 (1999).

[11] J. Stenger, S. Inouye, A.P. Chikkatur, D.M. Stamper-Kurn, D.E. Pritchard, and W. Ketterle, Phys. Rev. Lett. **82**, 4569 (1999).

[12] S. B. Papp, J.M. Pino, R.J. Wild, S. Ronen, C.E. Wieman, D.S. Jin, and E.A. Cornell, Phys. Rev. Lett. **101**, 135301 (2008).

[13] G. Veeravalli, E. Kuhnle, P. Dyke, and C.J. Vale, Phys. Rev. Lett. **101**, 250403 (2008).

[14] D. Clément, N. Fabbri, L. Fallani, C. Fort, and M. Inguscio, Phys. Rev. Lett. **102**, 155301 (2009).

[15] P. T. Ernst, S. Götze, J.S. Krauser, K. Pyka, D.-S. Lühmann, D. Pfannkuche, and K. Sengstock, Nat. Phys. **6**, 56 (2010).

[16] D.-I. Choi and Q. Niu, Phys. Rev. Lett. **82**, 2022(1999).

[17] M. Krämer, C. Menotti, L. Pitaevskii, and S. Stringari, Eur. Phys. J. D **27**, 247 (2003).

[18] X. Zhou, F. Yang, X. Yue, T. Vogt, and X. Chen, Phys. Rev. A **81**, 013615 (2010).

[19] O. Zobay and G.M. Nikolopoulos, Phys. Rev. A **73**, 013620 (2006).